

Numerical modelling of blue mussel (*Mytilus edulis*) bacterial contamination

Tomasz Dabrowski*, William J. Doré, Kieran Lyons, Glenn D. Nolan.

Marine Institute, Rinvilla, Oranmore, Co. Galway, Ireland

Corresponding author: Tomasz Dabrowski
Marine Institute, Rinvilla, Oranmore, Co. Galway, Ireland
E-mail: tomasz.dabrowski@marine.ie
Phone: +353 91 387367
Fax: +353 91 387201

Abstract

Bivalve shellfish such as oysters and mussels can concentrate human pathogens when grown in areas impacted by municipal wastewater. Under EU regulation this risk to consumers is controlled by determining the sanitary quality of bivalve shellfish production areas based on the concentration of *E. coli* present in shellfish flesh. The authors present a modelling approach to simulate an uptake of *E. coli* from seawater and subsequent depuration by *M. edulis*. The model that dynamically predicts *E. coli* concentration in the mussel tissue is embedded within a 3-D numerical modelling system comprising of a hydrodynamic, biogeochemical, shellfish ecophysiological and the newly proposed microbial modules. The microbial module has two state variables, namely, the concentrations of *E. coli* in water and in the mussel tissue. Novel formulations to calculate the filtration rates by mussels and the resulting uptake of bacteria are proposed; these rates are updated at every computational time step. Concentrations of *E. coli* in seawater are also updated accordingly taking into account the amounts ingested by mussels. The model has been applied to Bantry Bay in the south-west of Ireland. The results indicate that the model is capable of reproducing the official classification of shellfish waters in the bay based on monthly sampling at several stations. The predicted filtration rates and ratios of *E. coli* in water and mussels also compare well with the literature. The model thus forms a tool that may be used to assist in the classification of shellfish waters at much greater spatial and temporal detail than that offered by a field monitoring programme. Moreover, it can also aid in designing an efficient monitoring programme. The model can also be utilised to determine the contribution of individual point sources of pollution on the microbial loading in mussels and, when incorporated into an operational framework, it can provide a short-term forecasting of microbial contamination in a shellfishery. Also, the model can be easily extended to include other shellfish and pathogen species.

Keywords: numerical modelling; *Mytilus edulis*; DEB model; bacterial contamination; shellfish aquaculture.

1. Introduction

Bivalve shellfish such as oysters and mussels are filter-feeders and when grown in harvest areas impacted by sewage they can accumulate human pathogen. Such shellfish can present a significant health risk consumed raw or only lightly cooked. These risks are recognised internationally and regulations exist worldwide to control them. In European Union shellfish growing areas are classified into one of three categories based on the concentration of the faecal indicator organism *E. coli* present in shellfish flesh; these categories are defined in Table 1. The category determines the level of post harvest treatment required prior to sale for human consumption. These controls have been successful in virtually eliminating bacterial illness associated with bivalve shellfish. However, a number of outbreaks continue to be associated with the consumption of bivalve shellfish that are contaminated by human pathogenic viruses (Doré et al., 2010; Le Guyader et al., 2010; Lowther et al., 2012).

Several factors determine the level of bacterial contamination of bivalve filter-feeders. These can be grouped into factors determining coliform concentrations in ambient seawater and bivalve physiology. The former include physical transport processes, which determine travel times between the site and the source of contamination and the dilution of bacteria by mixing with seawater, and coliform die-off rates. Factors, which are typically considered when determining the die-off rates in seawater include solar radiation, temperature, salinity and suspended particulate matter concentration (e.g. Canteras et al., 1995; Chapra, 1997; Kashefipour et al., 2002; Yukselen et al., 2003). Due to differences in environmental conditions these rates can significantly vary both spatially and temporally even within one waterbody. Relevant processes determined by the bivalve physiology include the filtration and depuration rates. Filtration rates depend mainly on temperature, the availability of food and size of an animal (e.g. Gosling, 1992; van der Veer et al., 2006; Winter, 1973). Studies on depuration rates reveal that bacteria, including *E. coli*, are rapidly eliminated under suitable environmental conditions that are bivalve species-specific (Richards, 1998; Roderick and Schneider, 1994). Provided environmental conditions such as salinity, turbidity and dissolved oxygen concentrations are within an appropriate range, the principal factor influencing the rate of bacterial depuration is temperature (Lees et al., 2010).

Mathematical models describing the growth of various shellfish species and aiming at supporting the management of shellfish aquaculture have been developed over the last

c.20 years; recent examples include Ferreira et al. (2007, 2008), Filgueira and Grant (2009) and Nunes et al. (2011). The last decade saw an increase in the number and complexity of these models, and in recent years research efforts have intensified on the application of a Dynamic Energy Budget (DEB) theory (Kooijman, 2010) to modelling the growth and bioenergetics of bivalve filter-feeders. *Mytilus edulis*, amongst other species, has been successfully modelled using a DEB approach (e.g. Dabrowski et al., 2013; Handå et al., 2011; Filgueira et al., 2011; Maar et al., 2009; Rosland et al., 2009, 2011; Saraiva et al., 2011; Thomas et al., 2011; van der Veer et al., 2006). Several authors have dynamically coupled DEB models with biogeochemical models to provide feedbacks from aquaculture farms to phytoplankton and nutrient dynamics (e.g. Dabrowski et al., 2013; Grangeré et al., 2009, 2010; Guyondet et al., 2010; Maar et al., 2009; Ren et al., 2010 and other).

However, relatively few modelling approaches have been proposed to address bacterial contamination of cultured shellfish; these include studies by Fiandrino et al. (2003) for oysters farmed in Thau lagoon, France and by Martins et al. (2004) for clams harvested in Ria de Formosa, Portugal. In addition, none of the above studies fully accounts for the physiological response of bivalves to changing environmental conditions. In the former, the filtration rates depend on temperature and dry weight, without accounting for other factors, such as food availability, or are set constant based on laboratory and field experiments, as in the latter. It seems desirable then to have a general modelling tool integrating various components of an ecosystem and capable of simulating the level of bacterial contamination of shellfish in a dynamic natural environment. Such a model would enable estimating the level of bacterial contamination and the resulting classification of shellfish waters at the spatial and temporal detail that would be very difficult to achieve through the monitoring programme alone. Moreover, it would enable running numerous hypothetical scenarios involving, for example, new farms and outfalls or changes to the farming practices and sewage inputs. It would thus have a potential to be a very useful tool in the integrated coastal zone management aiding the decision making process for best locations for new aquaculture farms and sewage outfalls.

Such integrated modelling approach is presented in this paper. The authors present a new method to simulate an uptake of *E. coli* from seawater and subsequent depuration by *M. edulis* that dynamically predicts *E. coli* concentration in the mussel tissue. It is

embedded in a numerical model comprising of a physical, biogeochemical, shellfish ecophysiological and the newly proposed microbial modules. Details of the microbial module are presented in this paper together with the results from the application of the modelling system to Bantry Bay, Ireland.

2. Methods

2.1 Study site

The model was applied to Bantry Bay, located in the southwest of Ireland, which is one of the most important national regions for shellfish culture, and approximately 80% of national rope mussel is produced here and in the surrounding bays annually (Browne et al., 2008). Bantry Bay exhibits limited estuarine behaviour becoming thermally stratified in the summer months (Raine et al., 1990) with weak tidal currents, typically below 5 cm s^{-1} . When the bay is thermally stratified, variations in wind direction cause two layer oscillatory flows which generally result in the import of water from the near coastal continental shelf and in general water flushing is in an anticlockwise direction. Freshwater inputs to Bantry Bay are small and highly variable due to the mountainous character of the surrounding region. Five main rivers are Adrigole, Glengarriff, Coomhola, Owvane and Mealagh.

Main agglomerations on the shores of Bantry Bay are the towns of Bantry and Castletownbere. Effluents are secondary treated in wastewater treatment plant prior to discharging into the bay only in the case of the former. Several other smaller sources of sewage are distributed throughout the bay, as presented in Fig. 1; these are all untreated or primary treated sewage.

2.2 Modelling system components

The numerical model comprises of the hydrodynamic, biogeochemical, mussel ecophysiological, and, newly developed in this study, microbial modules. Fig. 2 presents a schematic overview of the modelling system components. Detailed description of the first three modules is available in Dabrowski et al. (2013) along with the coupling methodology and the validation report. Below, only a brief summary is provided. Subsequent section describes the microbial model and its integration with the system.

The 3D model of Bantry Bay used in this study is based on the Regional Ocean Modelling System (ROMS) which is a free-surface, hydrostatic, primitive equation

ocean model described in Shchepetkin and McWilliams (2005). ROMS uses orthogonal curvilinear coordinates on an Arakawa-C grid in the horizontal while utilizing a terrain-following (sigma) coordinate in the vertical. The model covers the area between 51N to 52N and 9W to 11W and is nested within two mesoscale models of the North East Atlantic, namely the ~2 km resolution hydrodynamic model and ~4 km resolution biogeochemical model. A computational mesh of horizontal resolution of 200-250m is used and in vertical it has 20 sigma levels. The hydrodynamic model prognostic variables are potential temperature, salinity, horizontal velocities and sea surface displacement.

The biogeochemical module is based on the nutrient-phytoplankton-zooplankton-detritus model (NPZD) developed by Fennel et al. (2006). The model state variables comprise of ammonium, nitrates, phytoplankton, chlorophyll *a*, zooplankton, small and large detritus and oxygen. Nitrogen is the primary unit used in the model, however, the phytoplankton, small and large detritus are also expressed in carbon units.

The mussel ecophysiological model is based on DEB theory and describes the uptake and utilisation of the energy by an organism throughout its lifecycle. The model has three state variables, namely the structural body volume, V , the energy reserves, E , and the reproductive energy, E_r . Two additional parameters are calculated from these state variables: shell length, L , and dry flesh weight, DW . This model provides feedback to the biogeochemical model that includes the following processes: food uptake and assimilation of nitrogen and carbon in bivalve, egestion of faeces, NH_4 excretion, oxygen utilization and CO_2 production; all formulations are provided in Dabrowski et al. (2013).

The modelling system comprising of the above components was previously applied to Bantry Bay and successfully reproduced the hydrodynamics, biogeochemical cycles and growth of rope mussel cultures in the bay (Dabrowski et al., 2013).

2.3 Microbial model

The authors developed a module that predicts a fate of *E. coli* in seawater following its point source input into the model, its uptake by *Mytilus edulis*, which also acts as a sink from water, and its concentration in mussel tissue. The following formulations are proposed.

Concentration of *E. coli* in water is determined by its die-off rate and the rate of uptake by mussels and is represented by a first-order equation:

$$\frac{dC_s}{dt} = -(k + 2.4 \cdot 10^4 k_u \cdot D_M) C_s \quad (1)$$

where C_s is *E. coli* concentration (CFU 100ml⁻¹), t is time (d), k is the *E. coli* decay rate in seawater (d⁻¹), k_u is the filtration rate of an individual bivalve (l g⁻¹ h⁻¹), $2.4 \cdot 10^4$ is the factor to convert the units of k_u to (100ml 100g⁻¹ d⁻¹), and D_M is the density of mussels in a given computational cell and expressed in (100g (wet weight) 100ml⁻¹). The formulation by Canteras et al. (1995), previously successfully used in numerical modelling of faecal pollution of the Estoril coast (Portugal) by Mateus et al. (2013), was adopted in this study to derive the value of k :

$$k = 2.533 \cdot 1.04^{(T-20)} \cdot 1.012^S + 0.113 i_z \quad (2)$$

where S and T are salinity (psu) and temperature (°C), respectively, and i_z is the shortwave radiation (watt m⁻²). S , T and i_z are computed by the model and defined on a 3D grid, and thus k is also computed for every model grid and updated every time step. Shortwave radiation applied in the model at the surface decreases exponentially with water depth at the rates dependent on water properties and chlorophyll concentration; see Fennel et al. (2006) for more details.

Concentration of *E. coli* in a mussel flesh, C_m (MPN 100g⁻¹; MPN – Most Probable Number), is governed by following equation:

$$\frac{dC_m}{dt} = 2.4 \cdot 10^4 k_u \cdot C_s - k_d \cdot C_m \quad (3)$$

where k_d is the depuration rate (d⁻¹). The depuration of bivalves is usually reported as T_{90} , the time in which 90% of population is no longer detectable. It can readily be shown that the relationship between T_{90} and k_d , assuming a first-order decay, is as follows:

$$k_d = \frac{2.303}{T_{90}} \quad (4)$$

In this study, the authors applied a T_{90} of 3 hrs following the findings of Doré and Lees (1995) for long-term exposure. This yields the value of $k_d = 18.4$ d⁻¹.

The authors derived an equation for k_u resulting from the energy ingestion rate predicted by the DEB model for *M. edulis*. The reader is referred to Dabrowski et al. (2013) for the DEB model formulations and its coupling to the biogeochemical model. As proposed in Dabrowski et al. (2013), the energy ingestion rate is converted to

carbon ingestion rate and its uptake in food is subsequently calculated. Phytoplankton is one of the food sources in the presented model; therefore k_u for an individual bivalve can be expressed as:

$$k_u = \frac{\dot{P}}{P \cdot V \cdot \rho} \quad (5)$$

where \dot{P} is phytoplankton uptake rate (mmol N h^{-1}), P is the concentration of phytoplankton biomass (mmol N l^{-3}), V is the volume of an individual bivalve (cm^3) and ρ is the specific density of *M. edulis* (g cm^{-3}), assumed equal 1 g cm^{-3} (Dabrowski et al., 2013). The value of k_u is multiplied by the number of individuals in a given computational cell prior to its application to eqs. (1) and (3).

2.4 Mussels *E. coli* contamination monitoring

Monthly samples of mussels were collected from designated locations throughout Bantry Bay as part of the national monitoring programme undertaken by the Competent Authority to determine the classification of shellfish harvest areas in Ireland. Mussels were transported to the laboratory under chilled conditions ($<15^\circ\text{C}$) and analysed for *E. coli* within 24 hrs of collection. Analysis was undertaken using the standard 5 tube 3 dilution most probable number (MPN) prescribed under EU regulation (Anon., 2005).

Shellfish area classification was determined by the national Competent Authority for each monitoring point based on EU regulatory limits (Table 1). The classifications were determined using data obtained over the proceeding three years 2009-2011. A category A or B classification was awarded if 90% of samples were ≤ 230 or $\leq 4,600$ MPN 100g^{-1} of shellfish flesh, respectively. In addition, a split classification between B and C was awarded where the monitoring demonstrated a clear seasonal pattern of contamination over the 3 year period consistent with category C ($\leq 46,000$ MPN 100g^{-1}) or category B ($90\% \leq 4,600$ MPN 100g^{-1}) at particular time of the year.

2.5 Description of the simulation

The simulation presented in this paper covers the time period of almost 1 year from 14 July 2010 to 28 June 2011, determined by the field data on mussel biometrics and environmental conditions that was acquired for validation of the mussel ecophysiological model. The initial size of the mussels distributed across the farms shown in Fig. 1 is c.3.3 cm, and at the end of June 2011 they reach shell lengths

varying from c.5.3 cm to 5.8 cm depending on the location. The numerical model was initialised by distributing appropriate number of individuals across the farms, in the corresponding numerical model cells in 3D (dropper lines are up to 8 m long), in proportion to farm sizes, and based on the estimated harvest in Bantry Bay of 3019 tonnes in 2011 and the average mussel weight of 7.8 g at the time of harvest. This translates to the mussel density ranging from c. 1 individual m^{-3} to over 20 individuals m^{-3} in most heavily cultivated areas. Full description of the shellfish ecophysiological model set-up can be found in Dabrowski et al. (2013).

Monitoring of the discharges and loadings is not taking place in Bantry Bay at present, therefore, in this modelling study the authors assumed constant dry weather flows based on population equivalent (PE) and *E. coli* concentrations that can be expected in treated and untreated sewage. Based on historical records of the Irish Environmental Protection Agency, the raw wastewater discharge from Bantry town prior to opening the existing Waste Water Treatment Plant (WWTP) was contributing $1.4 \cdot 10^6$ litres and $1.4 \cdot 10^{14}$ coliforms into the bay. This yields the *E. coli* concentration of $1 \cdot 10^7$ CFU 100ml^{-1} that the authors used for outfalls discharging untreated and primary only treated sewage. As regards, Bantry WWTP, the disinfection is not in place, therefore the coliforms removal rates are around 80% (typical for secondary treated sewage without disinfection); this gives the *E. coli* concentration of $2 \cdot 10^6$ CFU 100ml^{-1} . Locations of the outfalls across the bay are presented in Fig. 1. Table 2 summarizes the discharges and concentrations applied in the model. The outfalls in the model have been placed at the bottommost sigma level.

The output from the model is produced every 1 hour over the simulation time period. The initial two weeks of the simulation have been discarded allowing for the spin-up of the microbial model and the analysis commence on 1 August 2010. Subsequent section summarizes the results obtained.

3. Results

3.1 *E. coli* dispersion

In order to visualize a prevailing transport pattern of *E. coli* in the model from their sources, a ‘climatology’ map of *E. coli* concentrations was created by calculating an average of the predicted concentrations, C_s , over the simulation length and over the water column at each computational model cell. Fig. 3a presents the obtained spatial distribution of this mean in Bantry Bay. As can be seen, the *E. coli* concentration

decreases quickly when moving away from the outfalls, with the highest concentrations found in the immediate vicinity of the outfalls; of these the maximum is found at outfall No. 2 site and equals c.900 CFU 100ml⁻¹. In the case of the remaining outfalls, these concentrations are lower and vary from 80-320 CFU 100ml⁻¹. As regards the direction of plumes dispersion, the outfall No. 6 appears to affect more the areas upstream, where farms are located, whereas downstream the *E. coli* concentrations are lower most likely due to increased mixing with bay water. In general, sheltered areas around the Whiddy Island are affected by the discharges from the outfalls, whereas the concentrations in the exposed areas to the west of the island decrease quickly. The outfall No. 1 plume also reaches some of the farms nearby with the 'climatology' *E. coli* concentrations decreasing gradually with the distance from the outfall. The *E. coli* originating from the outfall No. 2 seem to mostly affect the farms located within the embayment with the concentration outside decreasing quickly.

Fig. 3b presents a map of the coefficient of variation, *CV*, of the average predicted *E. coli* concentration defined as the ratio of standard deviation to the average concentration. As can be seen, the distribution of *CV* is to a large extent an inverse of the distribution of the average *C_s*, with lowest values in the vicinity of the outfalls and greatest values away from the outfalls. For example, sites NC, SC and SE are characterized by *CV* in the region of 1-3, whereas sites GS, AE and SH by *CV* in excess of 8.

3.2 Mussel filtration rates

Water filtration rate by mussels is an important factor determining *C_m*. Since in the presented model its value changes at each model time step (30 s) and is determined based on coupled mussel eco-physiological and biogeochemical model predictions, it is important to ensure that the values of *k_u* returned by eq.(5) are reasonable. Fig. 4a presents the predicted *k_u* over 1 week in July 2010, November 2010 and June 2011, at monitoring station SE when the mussel shell lengths are c.3.3 cm, 4.5 cm and 5.5 cm, respectively. The availability of phytoplankton (expressed as chlorophyll *a*) also differs and changes from good (c.2.8 mg m⁻³) to very low (c.0.3 mg m⁻³) to moderate (c.1.0 mg m⁻³) in the selected time periods, respectively (see site SN01 in Dabrowski et al., 2013). The results indicate that there is a substantial variation in the predicted *k_u* between the selected time periods. In July 2010 *k_u* varies between 0.62 and 2.23 l g⁻¹

h^{-1} with the average of $1.16 \text{ l g}^{-1} \text{ h}^{-1}$. In November 2010 these values are higher and equal 1.21, 4.11 and $2.58 \text{ l g}^{-1} \text{ h}^{-1}$, respectively, whereas in June 2011 they are lowest and more stable at 0.30, 0.59 and $0.45 \text{ l g}^{-1} \text{ h}^{-1}$, respectively. Fig. 4b presents the corresponding hourly C_m values for the three time periods. As can be seen, C_m is highly variable and does not correlate with the filtration rates due to high variability of C_s (see the Discussion section where example values of *E. coli* decay rates given by eq. (2) are provided) and short T_{90} for C_m . For example, the predicted filtration rates on days 4-5 in November are up to six times greater than those on days 4-5 in July, and yet the predicted values of C_m are lower. The filtration rates are discussed further in the Discussion section.

3.3 Mussel contamination and predicted shellfish waters classes

Similar assessment methodology for determining shellfish waters classes to that described in Section 2.4 was applied to obtained model results; the difference lies in the number of ‘samples’ and the time period of the analysis. Considering the time period of almost 11 months (01 August – 28 June) and an hourly output from the model, the total of 7,969 values of C_m were obtained for each station. Table 3 summarizes obtained results and compares them with the results of the official shellfish waters monitoring programme and the classification awarded by the Competent Authority. With the exception of stations AE and GS, the model matches the official classification based on monthly sampling. In the model, all sources of *E. coli* are at considerable distance from the above two stations, whereas in reality the *E. coli* will enter the bay water from local inputs through streams and from diffuse sources following frequent rainfalls. Despite the assumptions made in relation to sewage discharges in this modelling study, the model is capable of reflecting the classification spanning from A to C at all remaining sites. The only Class C waters in Bantry Bay are those at station NC, the closest to the outfall No. 6. Also, notably, the model correctly predicts Class A waters at station CE, affected by the outfall No. 1, and station SH, affected by the outfalls upstream. All remaining sites fall into Class B category.

It is also desirable to know if the relative level of contamination at the sites is also reflected by the model. Fig. 5 presents normalized mean values of C_m for observational and modelled data; also shown are modelled normalized mean values of C_s . As regards C_m , the order of sites, with the exception of GF and CE is the same in

both datasets, with the relative contamination at the latter almost identical in the field samples and the model. The relative concentrations at GF as well as at SH are lower in the model compared to the observations; however, they are accurately reflected by the model at all remaining sites. Despite the assumptions made in this modelling study as regards the inputs of *E. coli*, the above results further confirm the predictive power of the presented model. A similar distribution of relative C_s concentrations is returned by the model, except for sites NC and SC, where, as opposed to C_m , the concentration at the latter is higher than at the former. The mean C_s distribution predicted by the model (see also Fig. 3) may therefore be used for general distinction between the relatively ‘good’ and relatively ‘bad’ sites, however they do not easily convert to C_m as will be presented and discussed in subsequent sections. The presented model aspires to be a tool for determining C_m as accurately as possible and for deriving shellfish waters classification rather than for identifying ‘good’ and ‘bad’ sites only. An important aspect of having well performing model is the ability to predict classification of shellfish waters at the farms not included in the monitoring programme. Fig. 6 presents the classification determined for all rope mussel farms in Bantry Bay using the same methodology as applied to the eight monitoring stations. As expected, the results show that the sites closest to the outfalls; namely the outfalls No. 6, 3 and 2, are Class C. Farms at further distances improve to Class B, followed by Class A. Fig. 6 also reveals that the areas close to the monitoring stations are not necessarily of the same class as at the station. For example, waters close to stations SC and SE are of Class C rather than B. Similarly, farms located to the west of CE station are in shellfish waters Class B rather than A. On the other hand the areas surrounding station GF are classified as A rather than B, with Class B returned by the model only at the computational cell corresponding to the station location. The above observations point that the model may prove a very useful tool supporting the design of the monitoring network.

It may also be of interest to examine the temporal variability of classification derived from the model predictions. Two time periods were considered, namely winter (October – March) and summer (April – September) and the results are summarized in Table 4. As can be seen, all stations (except AE and SH for reasons discussed) exhibit a clear seasonality in the classification, as it downgrades to one class lower in winter, and in the case of sites located closest to the outfalls (NC, SC and SE) it downgrades to Class C. Site GS, located at a considerable distance from the nearest outfall also

falls into class B in winter and it matches the official classification based on 3 years worth of monthly observations. It is worth noting that the only site that exhibits a clear seasonal pattern in the observational dataset is NC, classified as B in the period 01 December – 01 June and reverting to class C at other times. This is contrary to the model results, although slightly different time period was used. Possible reasons for such model behaviour across all sites are provided in the Discussion section. Finally, the predicted ratios of C_m to C_s were analyzed in this study for comparison with previously published figures. Concentrations of C_s lower than 1 CFU 100ml⁻¹ were excluded from the consideration, since these are reported as <1 CFU 100ml⁻¹ in the field data. Table 5 summarizes the ratios averaged over the simulation time period across the monitoring stations. The ratios are of the same order across all sites and, with the exception of GS, are fairly similar ranging from 2,240 at SE to 4,090 at CE. At GS this ratio is somewhat higher at 6,180 and is largely due to the hydrography of the region. As can be seen from Fig. 1, site GS is located at a considerable distance from the nearest outfall. Moreover, the general flushing of Bantry Bay is anticlockwise (Edwards et al., 1996), implying that this site is located upstream from the outfall No. 6. Moreover, as presented in Fig. 3b, site GS is characterized by distinctly higher intra-annual variability of C_s than the remaining sites. As the result, the outfall plume with $C_s > 1$ CFU 100ml⁻¹ reaches the site rarely and predominantly in winter when *E. coli* survival time is longer. Fig. 7 presents the C_m to C_s ratios at GS compared to the ratios averaged across all remaining sites throughout the simulation time period. As can be seen, the C_m to C_s ratios at GS are similar to those at the remaining sites for the same time. Since winter ratios are higher than the summer ones, hence higher value presented in Table 5 for site GS. C_m to C_s ratio is further discussed in sections 3.4 and 4.

3.4 Sensitivity of predicted C_m to C_s ratio to model parameters

A sensitivity test has been performed to evaluate the impact of T_{90} and the saturation coefficient for chlorophyll *a*, X_K , on the predicted C_m to C_s ratio. A standalone DEB model has been used in this analysis as computational requirements for running the complete modelling system are prohibitive. Two sets of simulations have been carried out representative of winter and summer conditions at two mussel sampling sites in Bantry, Snave and Gearhies, as regards the observed water temperatures and chlorophyll *a* concentrations. Winter season is defined as October-March, whereas

summer as April-October and the corresponding water temperatures equal 9.1 °C and 14.5 °C, and chlorophyll *a* 0.83 mg m⁻³ and 1.33 mg m⁻³, respectively (see Dabrowski et al. (2013) for details on sampling stations and collated data). The values of T_{90} were varied from 3 to 4.5 hours (see Doré and Lees (1995)) and of X_K from 0.41 to 3.3 (see Dabrowski et al. (2013)). The value of C_s was held constant and equal to 10⁷ CFU m⁻³. The initial shell length of 5 cm was chosen and the simulation was executed for 365 days. The first 30 days were discarded and the average C_m to C_s ratio was calculated over the remainder of the simulation time period. The uptake rates of *E. coli* by a mussel and expressed in CFU s⁻¹ were also calculated and averaged over the same time period. Table 6 summarizes the results obtained.

As can be seen in Table 6, both parameters significantly affect the obtained ratio. The impact of T_{90} is linear, i.e. 50% increase in the obtained ratio for T_{90} of 4.5 hours compared to T_{90} of 3 hours, as can be deduced from equation (3). Decrease of 61% and 53% in the values of the ratio is predicted for winter and summer conditions, respectively, when X_K is increased from 0.41 to 3.3. It is interesting to note that the ratios are very similar for $X_K = 1$ mg m⁻³ for both summer and winter conditions and the corresponding T_{90} despite the difference in environmental conditions. For $X_K < 1$ mg m⁻³ the winter ratios are greater than the summer ones, whereas for $X_K > 1$ mg m⁻³ they are lower. The predicted *E. coli* uptake rates help to interpret this observation. As can be seen in Table 6, these are always greater for the summer conditions compared to the corresponding winter conditions, as the energy ingestion rates, predicted by the DEB model are greater due to higher water temperature and better food availability. Significantly faster growth of a mussel in the summer for low X_K values compared to the winter conditions, with the final dry weights of 3.14 g and 1.98 g, respectively (for $X_K = 0.41$ mg m⁻³) explains the fact that the obtained C_m in the summer is lower, as it is given per unit weight. The actual *E. coli* uptake rates for winter and summer conditions and individual X_K values are also provided in Table 6.

4. Discussion

The presented numerical model comprising of four modules, namely, the hydrodynamic, biogeochemical, shellfish and microbial is capable of reproducing the official classification of shellfish waters in Bantry Bay, south-west Ireland, based on sampling carried out at eight stations. Spatial distribution of mussels bacterial contamination is also well reflected in the bay, as the order of sites from most to least

contaminated based on the long-term averages of the *E.coli* levels in mussel flesh is, with the exception of one site, the same in the model and field data. These results have been obtained despite some assumptions made in relation to the specification of *E. coli* sources, such as constant loadings through the existing outfalls at levels corresponding to the specific guidelines, lack of combined sewage overflows, lack of diffuse sources and inputs down the rivers and lack of field data on coliform concentrations in water to validate the seawater fate module. The above assumptions were made due to non-existence of relevant data for the studied region. Furthermore, although the numerical models are one of the most powerful tools for simulating marine environments at high spatial and temporal detail, they are not error-free, and the errors in predictions of the state variables in each module will propagate downstream in the modelling sequences; the microbial module presented in this study requires input from all three other modules. Nevertheless, the model is capable of reproducing the long-term average situation in the bay in relation to bacterial contamination of farmed mussels. Due to all the above, the obtained results give further confidence that the developed model is robust, and can be expected to return even more accurate predictions if more observational data on *E. coli* inputs and distribution is available. With the hydrodynamic and biogeochemical modules already run operationally at the Marine Institute it constitutes a promising tool for the development of a warning system for bacterial contamination of shellfish farms and grounds leading to exceedance of classification and health standards should this observational data become available in real-time. Furthermore, the model can be used to determine the likely impact of an individual point source of pollution on *E. coli* concentrations in a shellfish area. This provides a useful tool for regulators and treatment plant operators to determine the impact of existing or proposed individual wastewater treatment plants on *E. coli* concentrations in a shellfishery. Therefore, following the application of the model, the likelihood of an individual wastewater treatment plant allowing compliance with, or causing failure of, current regulatory limits can be assessed. Although the current model provides a useful tool for determining *E. coli* concentrations in mussels the modular approach adopted could allow it to be adapted for use to predict pathogen concentrations in bivalve shellfish. Norovirus is the most common agent associated with illness following bivalve shellfish consumption (Lees, 2000). Often these outbreaks have occurred even when shellfish are compliant with *E. coli* standards. Over the last few years increasing data

on the concentration of norovirus in the wastewater and shellfish has become available following the introduction of real-time quantitative PCR procedures (Flannery et al., 2012; Lowther et al., 2012; Nordgren et al., 2009). This data provide the basis of developing a norovirus pathogen module for use in the current model.

Further results presented in this study and allowing for maintaining good confidence in the choice of model formulations and the modelling approach include the obtained filtration rates and C_m to C_s ratios. As regards the filtration rates (eq. (5)), these are determined by the DEB feeding module, which is governed by a Holling's Type II response. Contrary to other modelling studies (e.g. Martins et al., 2004) and some theoretical considerations, where the filtration rates are frequently assumed constant, the filtration rates in the presented model are predicted dynamically and change with every model time step. The rates predicted by the presented model are within previously published values for the species of *Mytilus edulis*. The reader is referred to Cranford et al. (2011) for a comprehensive review of the filtration rate response to changes in physiological and environmental conditions for various bivalve filter feeders, including *M. edulis*.

As regards the C_m to C_s ratio, or the level of 'condensation' of *E. coli* in mussel flesh, Ho and Tam (2000) report these ratios to vary from 50-100 to 2,500. In the presented model the long-term average ratios are higher than the quoted upper limit, but still in the order of 10^3 . Some limited data collated from two sites in inner Bantry Bay in years 2004-2008 (*unpublished*) on quarterly basis indicates that this ratio can be anything from 1 to 6,000. Considering the above, the ratios in the model seem reasonable. In addition to X_K in the DEB model, there are two parameters in the presented model that can be assumed free and be used for calibration by the end-user; these are the depuration rate and the *E. coli* retention rate. As regards the former, the values of T_{90} equal to 3 hrs and 4.5 hrs were reported by Doré and Lees (1995) for long-term and short-term exposures by *M. edulis* to *E. coli*, respectively. Marino et al. (2005) also report the value of T_{90} of 3 hrs for the species of *M. galloprovincialis*. Depuration rates of other species can be different. For example Doré and Lees (1995) report the values of 6 and 6.5 hrs for long- and short-term exposures, respectively, for *C. gigas*. In this modelling study T_{90} of 3 hrs was chosen, however, it can be adjusted to any other value in other applications. In the idealized 0-dimensional sensitivity studies presented in section 3.4 the obtained ratios ranged from 388 to 1,665 for

various X_K , T_{90} , chlorophyll a concentrations and water temperatures. Moreover, an increase in *E. coli* uptake rates by mussels can be expected along with increasing water temperature and food concentration as also presented in Table 6 and discussed in section 3.4. It should be noted that due to linearity of the eq. (3), application of T_{90} of 4.5 hrs as opposed to 3 hrs will result in 50% increase in the predicted C_m values, under the same constant C_s concentrations and other parameters unchanged.

It can be further shown that the uptake rate of *E. coli* by mussels (first term on RHS of eq. (3)) can vary significantly in response to changing environmental conditions and mussel physiology. Let us consider two cases: case A, representing typical conditions in Bantry Bay's station SE at the peak of the summer ($T = 17^\circ\text{C}$, $S = 35$ psu, $i_{z0} = 526$ W m^{-2}), and case B at the peak of the winter ($T = 7.5^\circ\text{C}$, $S = 33$ psu, $i_{z0} = 170$ W m^{-2}). Values of k obtained from eq. (2) are thus 62.8 and 21.5, for summer and winter, respectively. Ignoring the 2nd term on RHS of eq. (1) for simplicity, it can be shown that the values of T_{90} equal 0.88 hrs and 2.6 hrs in cases A and B, respectively. Let us compare the uptake rates at time t equal to case A T_{90} . In case A $C_{st} = 0.1C_{s0}$, where C_{s0} is the initial *E. coli* concentration, whereas in case B $C_{st} = 0.45C_{s0}$. Assuming the worst case scenario, e.g. the maximum modelled k_u ($4.1 \text{ l g}^{-1} \text{ h}^{-1}$) in case B and the minimum modelled k_u ($0.3 \text{ l g}^{-1} \text{ h}^{-1}$) in case A (see Fig. 4 for k_u), the uptake rate derived from RHS of eq. (3) is 61.6 times higher in case B compared to case A. This is a significant difference in *E. coli* uptake rates further highlighting the predictive power of the presented model. It also shows that C_m and the resulting classification of shellfish waters cannot be easily derived from either conservative tracer dispersion studies or the *E. coli* seawater concentrations alone. This conclusion is further supported by highly variable C_m to C_s ratios obtained in this study (Fig. (7)) and the results presented in Fig. (5). As can be seen in Fig. (5), the mean *E. coli* concentrations at sites SC and CE are greater than at NC and GF, respectively, and yet they fall into higher shellfish waters class.

As far as the classification is concerned, it has been shown in this paper (see Table 4) that most sites downgrade to a class lower in the winter. This stems from the model formulations and set-up applied and is consistent with other results presented in this work, e.g. greater C_m to C_s ratios in winter and significantly slower *E. coli* decay rates in seawater under the winter conditions. It has previously been pointed that the model

uses guideline levels of *E. coli* in effluents and constant volumetric discharges based on population equivalent. These figures may depart from the actual inputs, which will also vary temporally. The model can thus be deemed reliable if it is capable of representing the official classification in the long-term, i.e. based on the entire simulation time period, which it does. A seasonal pattern observed in the model, which is not observed in the field data and in case of one site is contrary to the obtained results, points to the need of further tests and possible revision of the formulations used should details on *E.coli* inputs and higher frequency field observations become available. For example, the Bantry Bay region is a popular tourist destination, and thus greater effluent loadings to the bay in the summer can be expected. Also, frequent and irregular rainfalls may also introduce high temporal variability to the inputs of *E. coli* to the bay. The above factors are not accounted for in the present model.

The retention rate has not been mentioned in this paper, as 100% retention was assumed; see Cusson et al. (2005) for more comments. In general, for *M. edulis*, the smaller the size of particles the lower the retention rate with 100% retention observed for particles larger than 4 μm (Hawkins and Bayne, 1992). On the other hand, aggregation of coliforms contributes to the retention and assimilation of coliforms by mussels (Bernard, 1989), so the specification of appropriate retention rate is not a straightforward task. Nevertheless, a user-defined retention rate can be easily implemented in eqs. (1) and (3) allowing for the calibration of the model to fit the observations.

5. Conclusions

The presented model is a powerful tool capable of predicting shellfish waters classes across all shellfish farms and beds in cultured areas; this is virtually unachievable by running a field sampling programme alone. Also, the model can be used to design an efficient monitoring programme targeting the areas that are most prone to contamination. The model can also be used to determine the impact of individual wastewater treatment plants on the *E. coli* concentrations in a given shellfishery. Due to high spatial and temporal resolution of numerical models, very detailed picture of bacterial contamination in a given coastal waterbody can be delivered using this tool. The physical-biogeochemical components of the presented modelling system are run

at the Marine Institute operationally. Implementation of the remaining modules in the operational framework, providing that both real time inputs of *E. coli* and estimates of mussel standing stocks are available may prove a very useful short-term forecasting system that will advise the aquaculture industry about the levels of expected bacterial contamination. It may significantly improve the operations of the farms as, for example, harvesting may be postponed for certain time period allowing the mussels to depurate naturally in order to avoid time-consuming and costly post-processing of harvested contaminated bivalves.

One of the advantages of using a DEB ecophysiological model in the presented system lies in a generic nature of its formulations meaning an ease of its adaptation to modelling other bivalve species provided that appropriate parameterization is applied. The presented model for *E. coli* should also work well with other bivalve species provided that the depuration rates are known. Furthermore, it can be easily extended to modelling other pathogens, such as noroviruses and bacteriophages, and their uptake by shellfish.

Acknowledgments

This study was funded by the EU Interreg IVB Atlantic Area Programme and was part of the EASYCO (Collaborative European Atlantic Water Quality Forecasting System) project. The authors wish to acknowledge the Sea Fisheries Protection Authority, Ireland, for providing data on *E. coli* contamination and classification of shellfish waters in Bantry Bay.

References

- Anonymous, 2005. ISO/TS 16649-3 Microbiology of food and animal feeding stuffs- Horizontal method for the enumeration of B-glucuronidase-positive *Escherichia coli* - Part 3: Most probable number technique using 5-bromo-4-chloro-3-indolyl-B-D-gucuronide.
- Bernard, F.R., 1989. Uptake and elimination of coliform bacteria by four marine bivalve mollusks. Canadian Journal of Fisheries and Aquatic Sciences 46(9), 1592-1599.
- Browne, R., Deegan, B., Watson, L., MacGiolla Bhríde, D., Norman, M., Ó'Cinnéide, M., Jackson, D., O'Carroll, T., 2008. Status of Irish Aquaculture 2007. Report by

- Marine Institute, Bor Iascaigh Mhara and Údarás na Gaeltachta. December 2008, 142pp.
- Canteras, J.C., Juanes, J.A., Perez, L., Koev, K.N. 1995. Modeling the coliforms inactivation rates in the Cantabrian Sea (Bay of Biscay) from *in situ* and laboratory determinations of T₉₀. Water Science and Technology 32(2), 37-44.
- Chapra, S.C., 1997. Surface water-quality modeling, McGraw-Hill, New York, 1997. 844pp.
- Cranford, P.J., Ward, J.E., Shumway, S.E., 2011. Bivalve filter feeding: variability and limits of the aquaculture biofilter, in: Shumway, S.E. (Ed.), Shellfish Aquaculture and the Environment, First Edition. John Wiley & Sons, Inc., Ames, Iowa, pp. 81-124.
- Cusson, M., Tremblay, R., Daigle, G., Roussy, M., 2005. Modeling the depuration potential of blue mussels (*Mytilus* spp.) in response to thermal shock. Aquaculture 250, 183-193.
- Dabrowski, T., Lyons, K., Curé, M., Berry, A., Nolan, G., 2013. Numerical modelling of spatio-temporal variability of growth of *Mytilus edulis* (L.) and influence of its cultivation on ecosystem functioning. Journal of Sea Research 76, 5-21.
- Doré, W.J., Lees, D.N., 1995. Behavior of *Escherichia coli* and Male-Specific Bacteriophage in Environmentally Contaminated Bivalve Molluscs before and after Depuration. Applied and Environmental Microbiology 61(8), 2830-2834.
- Doré, B., Keaveney, S., Flannery, J., Rajko-Nenow, P., 2010. Management of health risk associated with oysters harvested from a norovirus contaminated area, Ireland, February - March 2010. EuroSurveillance 15, 1-5.
- Fennel, K., Wilkin, J., Levin, L., Moisan, J., O'Reilly, J., Haidvogel, D., 2006. Nitrogen cycling in the Middle Atlantic Bight: Results from a three-dimensional model and implications for the North Atlantic nitrogen budget. Global Biogeochemical Cycles 20: GB3007 doi:10.1029/2005GB002456.
- Ferreira, J.G., Hawkins, A.J.S., Bricker, S.B., 2007. Management of productivity, environmental effects and profitability of shellfish aquaculture - the Farm Aquaculture Resource Management (FARM) model. Aquaculture 264, 160-174.
- Ferreira, J.G., Hawkins, A.J.S., Monteiro, P., Moore, H., Service, M., Pascoe, P.L., Ramos, L., Sequeira, A., 2008. Integrated assessment of ecosystem-scale carrying capacity in shellfish growing areas. Aquaculture 275, 138-151.
- Filgueira, R., Grant, J., 2009. A box model for ecosystem-level management of mussel culture carrying capacity in a coastal Bay. Ecosystems 12, 1222-1233.
- Fiandrino, A. Martin, Y., Got, P., Bonnefont, J.L., Troussellier, M., 2003. Bacterial contamination of Mediterranean coastal seawater as affected by riverine inputs:

- simulation approach applied to a shellfish breeding area (Thau lagoon, France). *Water Research* 37, 1711-1722.
- Filgueira, R., Rosland, R., Grant, J., 2011. A comparison of scope for growth (SFG) and dynamic energy budget (DEB) models applied to the blue mussel (*Mytilus edulis*). *Journal of Sea Research* 66(4), 403-410.
- Flannery, J., Keaveney, S., Rajko-Nenow, P., O'Flaherty, V., Doré, W., 2012. Concentration of Norovirus during Wastewater Treatment and Its Impact on Oyster Contamination. *Applied and Environmental Microbiology* 78, 3400-6.
- Gosling, E., 1992. The Mussel *Mytilus*: ecology, physiology, genetics and culture. *Developments in Aquaculture and Fisheries Science*, 25, Elsevier, Amsterdam, 1992. 589pp.
- Grangeré, K., Ménesguen, A., Lefebvre, S., Bacher, C., Pouvreau, S., 2009. Modelling the influence of environmental factors on the physiological status of the Pacific oyster *Crassostrea gigas* in an estuarine embayment; The Baie des Veys (France). *Journal of Sea Research* 62(2-3), 147-158.
- Grangeré, K., Lefebvre, S., Bacher, C., Cugier, P., Ménesguen, A., 2010. Modelling the spatial heterogeneity of ecological processes in an intertidal estuarine bay: dynamic interactions between bivalves and phytoplankton. *Marine Ecology Progress Series* 415, 141-158.
- Guyondet, T., Roy, S., Koutitonsky, V.G., Grant, J., Guglielmo, T., 2010. Integrating multiple spatial scales in the carrying capacity assessment of a coastal ecosystem for bivalve aquaculture. *Journal of Sea Research* 64, 341-359.
- Handå, A., Alver, M., Edvardsen, C.V., Halstensen, S., Olsen, A.J., Øie, G., Reitan, K.I., Olsen, Y., Reinertsen, H., 2011. Growth of farmed blue mussel (*Mytilus edulis* L.) in a Norwegian coastal area; comparison of food proxies by DEB modeling. *Journal of Sea Research* 66(4), 297-307.
- Hawkins, A.J.S., Bayne, B.L., 1992. Physiological interrelations, and the regulation of production, in: Gosling, E. (ed.), *The Mussel Mytilus: ecology, physiology, genetics and culture*. *Developments in Aquaculture and Fisheries Science* 25. Elsevier, Amsterdam, pp. 171-222.
- Ho, B.S.W., Tam, T.-Y., 2000. Natural depuration of shellfish for human consumption: a note of caution. *Water Research* 34(4), 1401-1406.
- Kashefipour, S.M., Lin, B., Harris, E., Falconer, R.A., 2002. Hydro-environmental modelling for bathing water compliance of an estuarine basin. *Water Research* 36, 1854-1868.
- Kooijman, S.A.L.M., 2010. *Dynamic Energy Budget Theory for Metabolic Organisation*, 3rd edition. Cambridge University Press, Cambridge, 2010. 514pp.
- Le Guyader, F.S., Krol, J., Ambert-Balay, K., Ruvoen-Clouet, N., Desaubliaux, B., Parnaudeau, S., Le Saux, J.C., Ponge, A., Pothier, P., Atmar, R.L., Le Pendu, J.,

2010. Comprehensive Analysis of a Norovirus-Associated Gastroenteritis Outbreak from the Environment to the Consumer. *Journal of Clinical Microbiology* 48, 915-920.
- Lees, D., 2000. Viruses and bivalve shellfish. *International Journal of Food Microbiology* 59, 81-116.
- Lees, D., Younger, A., Doré, B. 2010. Depuration and relaying. In: G. Rees, K. Pond, D. Kay, B. J. and J. Santo Domingo (Eds), *Safe management of shellfish and harvest waters*. International Water Association, London. pp.145-181.
- Lowther, J.E., Gustar, N.E., Powell, A.L., Hartnell, R.E., Lees, D.N., 2012. A two-year systematic study to assess norovirus contamination in oysters from commercial harvesting areas in the United Kingdom. *Applied and Environmental Microbiology*.
- Lowther, J.A., Gustar, N.E., Hartnell, R.E., Lees, D.N., 2012. Comparison of norovirus RNA levels in outbreak-related oysters with background environmental levels. *Journal of Food Protection* 75, 389-393.
- Maar, M., Bolding, K., Petersen, J.K., Hansen, J.L.S., Timmermann, K., 2009. Local effects of blue mussels around turbine foundations in an ecosystem model of Nysted off-shore wind farm, Denmark. *Journal of Sea Research* 62(2-3), 159-174.
- Marino, A., Lombardo, L., Fiorentino, C., Orlandella, B., Monticelli, L., Nostro, A., Alonzo, V., 2005. Uptake of *Escherichia coli*, *Vibrio cholerae* non-OI and *Enterococcus durans* by, and depuration of mussels (*Mytilus galloprovincialis*). *International Journal of Food Microbiology* 99, 281-286.
- Martins, F., Reis, M.P., Neves, R., Cravo, A.P., Brito, A., Venâncio, A., 2004. Molluscan shellfish bacterial contamination in Ria Formosa coastal lagoon: A modelling approach. *Journal of Coastal Research* SI 39, 1551-1555.
- Mateus, M., Pina, P., Coelho, H., Neves, R., Leitão, P.C., 2013. Faecal pollution modelling as a management tool in coastal areas: a case study in Estoril, Portugal, in: Mateus, M., Neves, R. (Eds.), *Ocean modelling for coastal management: Case studies with MOHID*. IST Press, Lisbon, pp. 83-95.
- Nordgren, J., Matussek, A., Mattsson, A., Svensson, L., Lindgren, P.E., 2009. Prevalence of norovirus and factors influencing virus concentrations during one year in a full-scale wastewater treatment plant. *Water Research* 43, 1117-1125.
- Nunes, J.P., Ferreira, J.G., Bricker, S.B., O'Loan, B., Dabrowski, T., Dallaghan, B., Hawkins, A., O'Connor, B., O'Carroll, T., 2011. Towards an ecosystem approach to aquaculture: Assessment of sustainable shellfish cultivation at different scales of space, time and complexity. *Aquaculture* 315, 369-383.
- Raine, R., McMahon, T., O'Mahoney, J., Moloney, M. and Roden, C. 1990. Water circulation and phytoplankton populations in two estuaries on the west coast of

- Ireland, in: Chambers, P. L., Chambers, C. M. (Eds.), Estuarine Ecotoxicology. JAPAGA, Wicklow, Ireland, pp. 19-28.
- Ren, J.S., Ross, A.H., Hadfield, M.G., Hayden, B.J., 2010. An ecosystem model for estimating potential shellfish culture production in sheltered coastal waters. Ecological Modelling 221, 527-539.
- Richards, G.P., 1988. Microbial purification of shellfish a review of depuration and relaying. Journal of Food Protection 51, 218-251.
- Roderick, G.E., Schneider, K.R., 1994. Depuration and Relaying of Molluscan Shellfish. In: C.R. Hackney and M.D. Pierson (Eds), Environmental Indicators and Shellfish Safety. Chapman & Hall, New York, USA., pp. 331-363.
- Rosland, R., Strand, Ø., Alunno-Bruscia, M., Bacher, C., Strohmeier, T., 2009. Applying Dynamic Energy Budget (DEB) theory to simulate growth and bio-energetics of blue mussels under low seston conditions. Journal of Sea Research 62(2-3), 49-61.
- Rosland, R., Bacher, C., Strand, Ø., Aure, J., Strohmeier, T., 2011. Modelling growth variability in longline mussel farms as a function of stocking density and farm design. Journal of Sea Research 66(4), 318-330.
- Saraiva, S., van der Meer, J., Kooijman, S.A.L.M., Sousa, T., 2011. DEB parameters estimation for *Mytilus edulis*. Journal of Sea Research 66(4), 289-296.
- Shchepetkin, A.F., McWilliams, J.C., 2005. The regional oceanic modeling (ROMS): a split-explicit, free-surface, topography-following-coordinate oceanic model. Ocean Modelling 9, 347-404.
- Thomas, Y., Mazurié, J., Alunno-Bruscia, M., Bacher, C., Bouget, J.-F., Gohin, F., Pouvreau, S., Struski, C., 2011. Modelling spatio-temporal variability of *Mytilus edulis* (L.) growth by forcing a dynamic energy budget model with satellite-derived environmental data. Journal of Sea Research 66(4), 308-317.
- van der Veer, H.W., Cardoso, J.F.M.F., van der Meer, J., 2006. The estimation of DEB parameters for various Northeast Atlantic bivalve species. Journal of Sea Research 56, 107-124.
- Winter, J.E., 1973. The filtration rate of *Mytilus edulis* and its dependence on algal concentration measured by a continuous automatic recording apparatus. Marine Biology 22, 317-328.
- Yukselen, M.A., Calli, B., Gokyay, O., Saatci, A., 2003. Inactivation of coliform bacteria in Black Sea waters due to solar radiation. Environment International 29(1), 45-50.

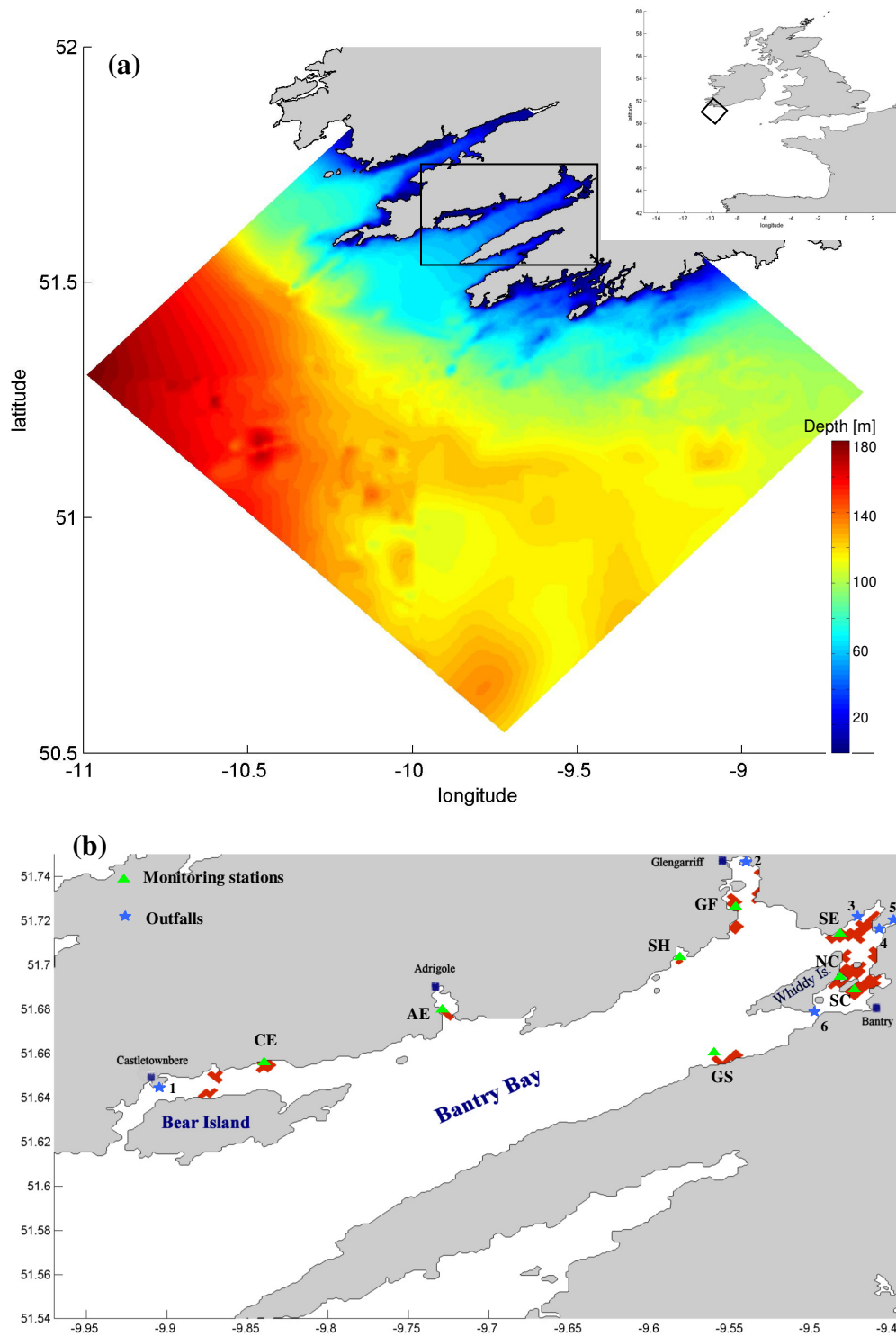


Figure 1. Maps showing the (a) bathymetry and extents of the numerical model of SW coast of Ireland and (b) distribution of rope mussel farms (red polygons) in Bantry Bay, locations of outfalls and locations of mussels bacterial contamination monitoring stations.

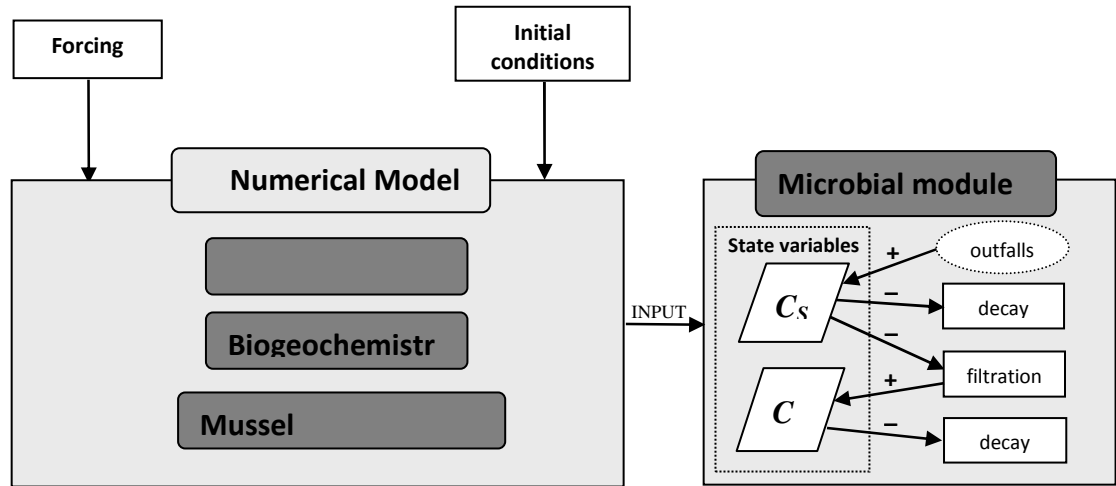


Figure 2. A schematic diagram of an integration of a newly developed microbial module with a numerical model. Symbols are: C_s – *E. coli* concentration in seawater, C_m – *E. coli* concentration in mussel flesh, ‘+’ represents a source, ‘-’ represents a sink.

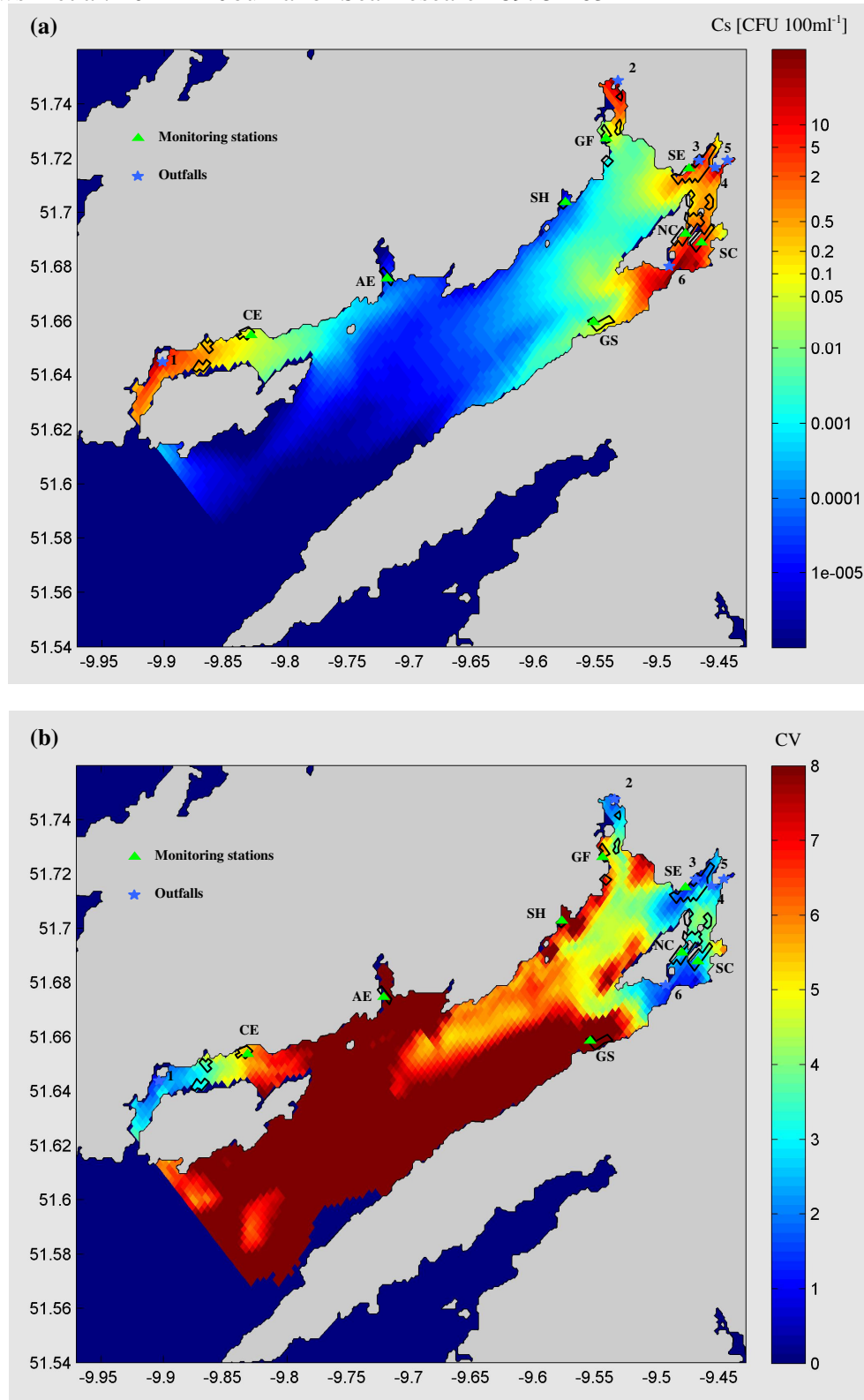


Figure 3. (a) Average predicted *E. coli* concentrations in Bantry Bay over the simulation time period, (b) coefficient of variation (CV) of the average predicted *E. coli* concentrations.

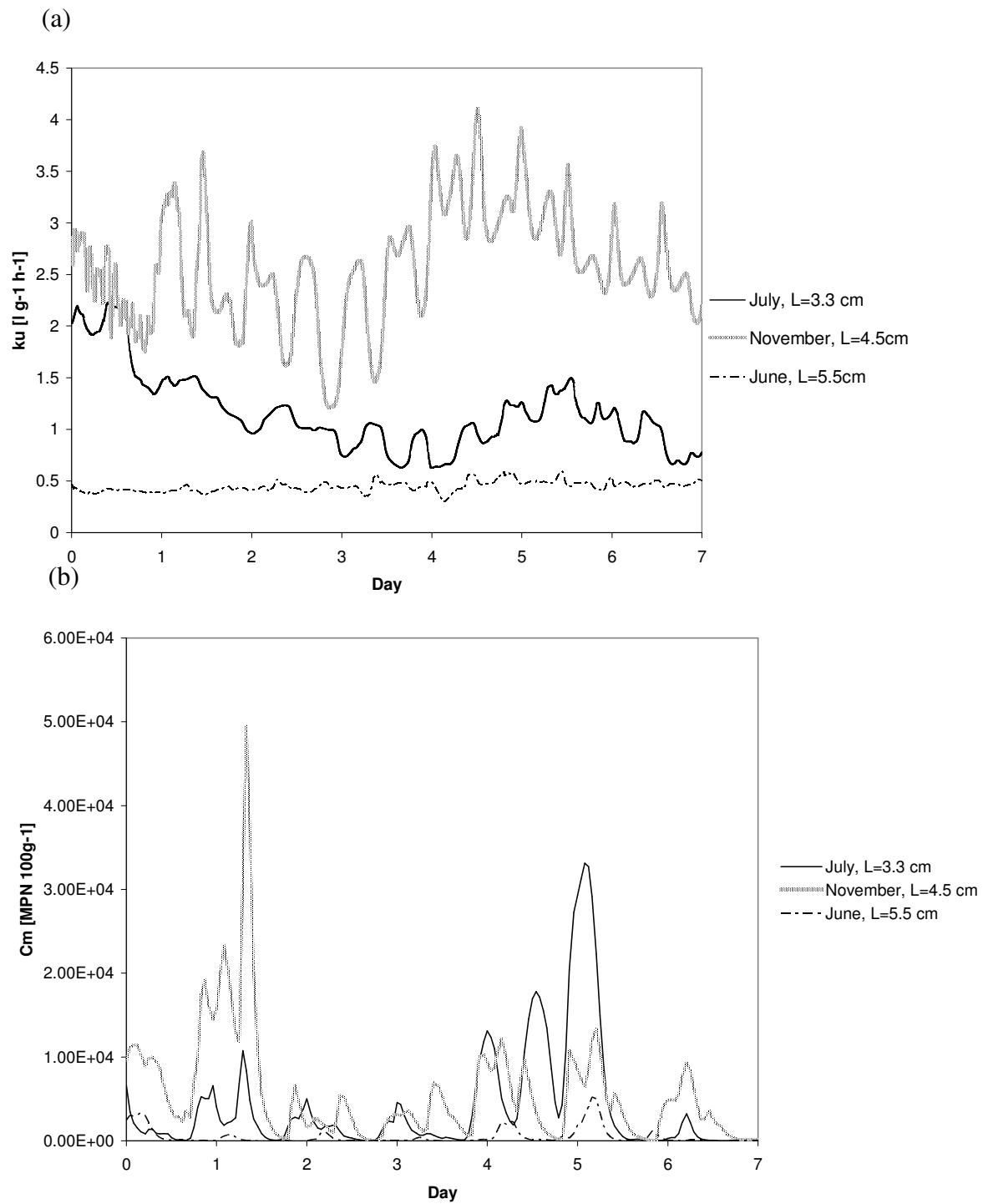


Figure 4. (a) Predicted filtration rates by an individual mussel and (b) corresponding C_m concentrations at surface layer at site SE.

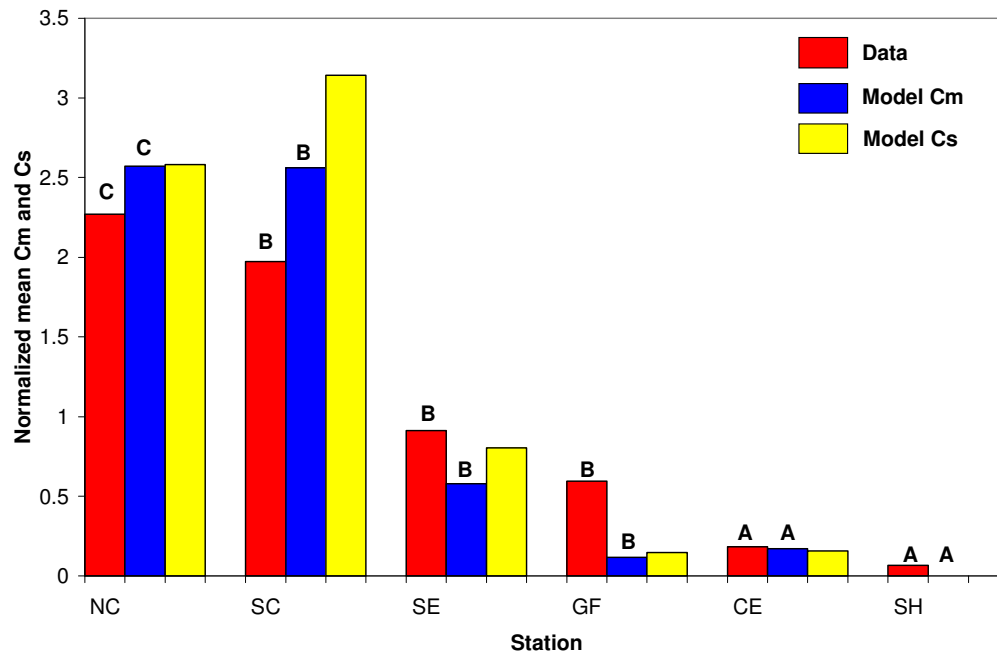


Figure 5. Normalized mean values of *E. coli* concentrations in mussels tissue and water. Normalized values were obtained by dividing the mean at each station by the mean across all stations.

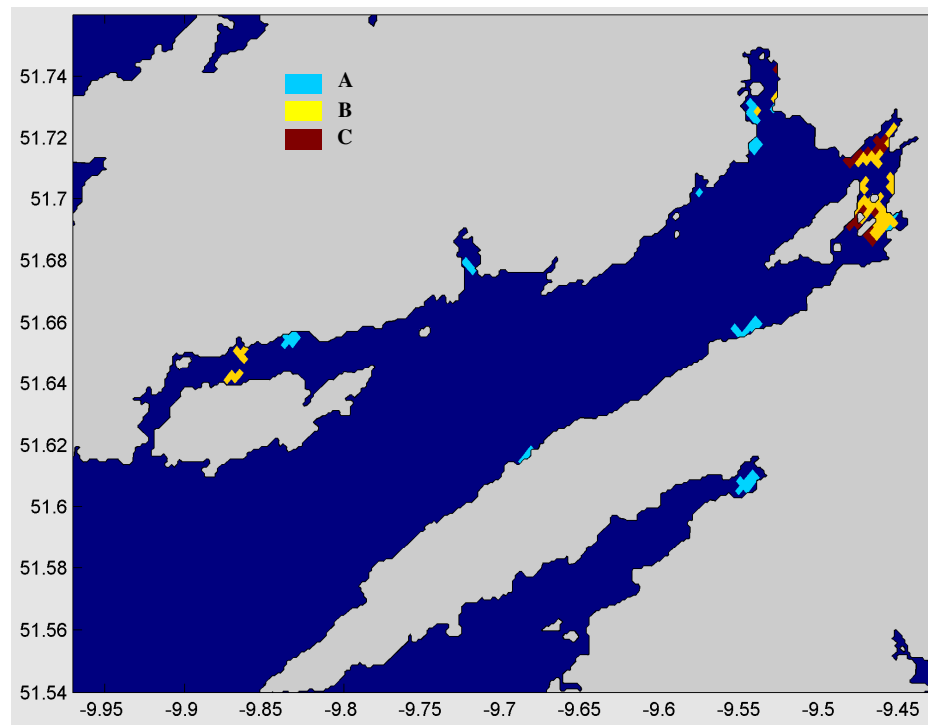


Figure 6. Shellfish waters classification in Bantry Bay predicted by the model.

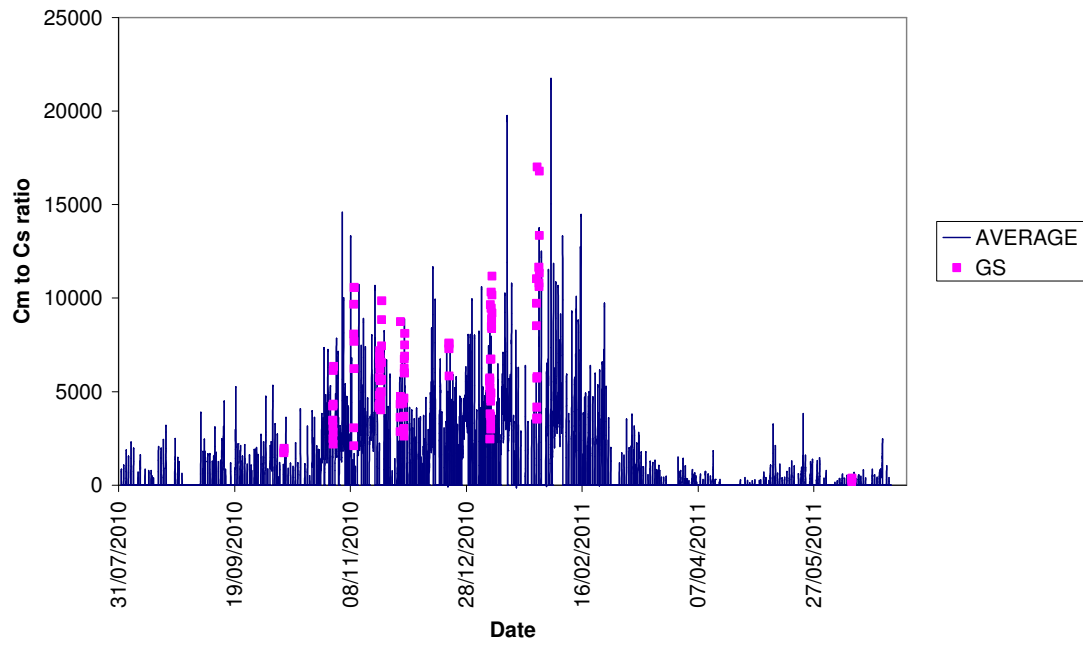


Figure 7. Timeseries of C_m to C_s ratio at station GS compared to the ratio averaged across all remaining sites.

Table 1. Classification criteria for shellfish harvesting areas.

Category	E. coli level (MPN 100g ⁻¹)	Treatment required
Class A	<230	May go for direct human consumption
Class B	<4,600	Must be depurated, heat treated or relayed to meet Class A requirements
Class C	<46,000	Must be relayed for 2 months to meet Class A or Class B requirements – may also be heat treated

Table 2. Volumetric discharges and *E. coli* in effluents entering Bantry Bay.

Name	Symbol	Discharge (m ³ d ⁻¹)	<i>E. coli</i> (CFU 100ml ⁻¹)
Castletownbere	CE	292.5	1·10 ⁷
Glengariff	GF	247.5	1·10 ⁷
Ardnagashel	AG	40*	1·10 ⁷
Eagle Point	EP	100	1·10 ⁷
Ballylickey	BL	40	1·10 ⁷
Bantry	BY	1,381	2·10 ⁶

* Seasonal only: May-September.

Table 3. Comparison of the classification of shellfish waters to model-derived classification in Bantry Bay.

Station	Category	Number of samples		Percentage of total [%]		Class	
		Data	Model	Data	Model	Data	Model
CK-BB-CE	A	36	7450	92	93.5	A	A
	B	3	391	8	4.9		
	C	0	128	0	1.6		
CK-BB-AE	A	22	7969	71	100	B	A
	B	7	0	23	0		
	C	2	0	6	0		
CK-BB-SH	A	18	7969	95	100	A	A
	B	1	0	5	0		
	C	0	0	0	0		
CK-BB-GF	A	27	7077	77	88.8	B	B
	B	7	826	20	10.4		
	C	1	66	3	0.8		
CK-BB-SE	A	24	4201	71	52.7	B	B
	B	8	3260	24	40.9		
	C	2	508	6	6.4		
CK-BB-NC	A	23	5410	70	67.9	C*	C
	B	6	1725	18	21.6		
	C	4	834	12	10.5		
CK-BB-SC	A	19	6100	56	76.5	B	B
	B	12	1146	35	14.4		
	C	3	724	9	9.1		
CK-BB-GS	A	24	7422	83	93.1	B	A
	B	5	423	17	5.3		
	C	0	134	0	1.5		

* Seasonal B 01 Dec – 01 Jun, reverts to class C at other times

Table 4. Seasonal classification of shellfish waters in Bantry Bay based on model results (winter: October – March, summer: April – September).

Station	Category	Percentage of predictions [%]		Class	
		Winter	Summer	Winter	Summer
CE	A	88.3	99.8	B	A
	B	8.8	0.2		
	C	2.9	0		
AE	A	100	100	A	A
	B	0	0		
	C	0	0		
SH	A	100	100	A	A
	B	0	0		
	C	0	0		
GF	A	79.9	99.7	B	A
	B	18.6	0.3		
	C	1.5	0		
SE	A	33.7	75.8	C	B
	B	54.8	24.1		
	C	11.5	0.1		
NC	A	52.8	86.2	C	B
	B	30.2	11.3		
	C	17.1	2.5		
SC	A	66.2	89.1	C	B
	B	19	8.8		
	C	14.8	2.1		
GS	A	87.7	99.7	B	A
	B	9.5	0.3		
	C	2.8	0		

Table 5. Ratios of *E. coli* seawater to mussel flesh concentrations averaged over the simulation time period.

Station	C_s / C_m
CE	4,090
AE	N/A
SH	N/A
GF	2,640
SE	2,240
NC	3,360
SC	2,860
GS	6,180

Table 6. Results from the sensitivity studies of C_m to C_s ratio to the values of T_{90} and X_K for summer ($T = 14.1^\circ\text{C}$, chlorophyll $a = 1.33 \text{ mg m}^{-3}$) and winter ($T = 9.5^\circ\text{C}$, chlorophyll $a = 0.83 \text{ mg m}^{-3}$) conditions. Also shown are *E. coli* uptake rates by a mussel.

$\begin{matrix} T_{90} \\ X_K \end{matrix}$	C_m to C_s ratio [-]								<i>E. coli</i> uptake [CFU s ⁻¹]	
	Summer				Winter				Summer	Winter
	3	3.5	4	4.5	3	3.5	4	4.5		
0.41	989	1150	1320	1483	1110	1300	1480	1665	10.3	8.8
1.0	813	949	1084	1219	828	967	1110	1242	6.2	4.9
1.5	714	833	952	1071	675	788	902	1012	4.5	3.6
2.0	635	741	847	952	561	655	750	841	3.5	2.9
2.5	559	652	745	838	479	559	640	718	2.9	2.4
3.3	467	545	622	700	388	453	518	582	2.4	1.9